XI International Conference on Computational Plasticity. Fundamentals and Applications
COMPLAS XI
E. Oñate, D.R.J. Owen, D. Peric and B. Suárez (Eds)

NUMERICAL IMPLEMENTATION OF A GENERALIZED PLASTICITY MODEL AT FINITE STRAINS

FABIO DE ANGELIS*, **ROBERT L. TAYLOR**†

*Department of Structural Engineering
University of Naples Federico II
Naples, Italy
e-mail: fabio.deangelis@unina.it

†Department of Civil and Environmental Engineering
University of California, Berkeley
Berkeley, CA 94720-1710, USA
e-mail: rlt@ce.berkeley.edu

Key words: Generalized Plasticity, Finite Element Method, Computational Algorithms

Abstract. In the present paper an algorithmic implementation of a generalized plasticity model is presented with reference to a material behaviour at finite strains. A return mapping algorithm is implemented for an elastoplastic material behaviour in large deformations. A computationally efficient algorithmic scheme is described and the performance of a generalized plasticity model at finite deformations is illustrated. Numerical results and examples are finally reported.

1 INTRODUCTION

The simulation and numerical treatment of the evolutive problem in elastoplasticity has become nowadays an important topic in the literature. Significant progress has been achieved over the last decades both in the mathematical comprehension of the problem and in the related computational treatment. At present, the algorithmic procedures have acquired significant improvements in the integration of the boundary value problem in elastoplasticity, see among others Simo and Hughes [1] and Zienkiewicz and Taylor [2]. However, in order to describe the observed behaviour of solids which are plastically loaded, unloaded, and then reloaded, it is necessary for the model to exhibit renewed plasticity prior to the state at which unloading initially occurred. With this perspective a generalized plasticity model was originally developed by Lubliner [3] [4]. Subsequently, a new model of generalized plasticity was proposed by Lubliner et al. [5] with the aim of including refinements for improved numerical implementation performances. An analysis of the numerical properties of the generalized plasticity model was illustrated by Auricchio and Taylor [6] for the case of elastoplasticity at infinitesimal strains. In the mentioned paper a comparative analysis is also reported with respect to other types of plasticity models which are classically adopted in the literature.

In the present paper a generalized plasticity model is described in a finite deformation setting and the characteristics of the generalized plasticity model at finite deformations are illustrated. An algorithmic scheme is presented for the numerical integration of the generalized plasticity model in the context of elastoplasticity at finite strains. A return mapping algorithm is described for an elastoplastic material behaviour in large deformations. The computational performance of the algorithmic scheme and its numerical integration features are reported. Numerical results and examples are finally presented in order to illustrate the effectiveness of the proposed solution scheme for the numerical integration of the generalized plasticity model in the simulation of inelastic processes at finite deformations.

2 CONTINUUM PROBLEM AND CONSTITUTIVE EQUATIONS

A local multiplicative decomposition of the deformation gradient $\mathbf{F}$ is considered in the form (Lee [7], Mandel [8])

$$\mathbf{F} = \mathbf{F}^e \mathbf{F}^p \tag{1}$$

where $\mathbf{F}^e$ and $\mathbf{F}^p$ respectively represent the elastic and plastic part of the deformation gradient. The elastic right Cauchy-Green tensor $\mathbf{C}^e$ and the elastic left Cauchy-Green tensor $\mathbf{b}^e$ are defined as

$$\begin{aligned} \mathbf{C}^e &= \mathbf{F}^{e,T}\,\mathbf{F}^e \\ \mathbf{b}^e &= \mathbf{F}^e\,\mathbf{F}^{e,T} \end{aligned} \tag{2}$$

where the superscript T indicates the transpose. We also consider $\mathbf{b}^e$ as expressed by (Simo and Hughes [1])

$$\mathbf{b}^e = \mathbf{F}\mathbf{C}^{p-1}\mathbf{F}^T, \tag{3}$$

where the plastic right Cauchy-Green tensor $\mathbf{C}^p$ is defined as

$$\mathbf{C}^p = \mathbf{F}^{p,T}\mathbf{F}^p. \tag{4}$$

The free energy ψ is expressed as an isotropic function

$$\psi = \hat{\psi}(\mathbf{b}^e, \boldsymbol{\xi}), \tag{5}$$

where $\boldsymbol{\xi}$ is a kinematic internal variable, and the Kirchhoff stress $\boldsymbol{\tau}$ is given by

$$\boldsymbol{\tau} = 2\frac{\partial \psi}{\partial \mathbf{b}^e}\mathbf{b}^e. \tag{6}$$

As a result of the restriction to isotropy the principal directions of the Kirchhoff stress and of the elastic left Cauchy-Green tensor coincide and therefore, by indicating with $\mathbf{n}_A$ such principal directions, a spectral decomposition is introduced as

$$\boldsymbol{\tau} = \sum_{A=1}^{3} \tau_A \, \mathbf{n}_A \otimes \mathbf{n}_A,$$
$$\mathbf{b}^e = \sum_{A=1}^{3} (\lambda_A^e)^2 \, \mathbf{n}_A \otimes \mathbf{n}_A. \tag{7}$$

Equation (6) therefore reduces to

$$\tau_A = 2\frac{\partial \psi}{\partial[(\lambda_A^e)^2]}(\lambda_A^e)^2. \tag{8}$$

The Kirchhoff stress is split into its volumetric and deviatoric parts as

$$\boldsymbol{\tau} = p\mathbf{1} + \mathbf{t} \tag{9}$$

where $\mathbf{1}$ is the second order identity tensor, $p \overset{\text{def}}{=} (\boldsymbol{\tau} : \mathbf{1})/3$ is the pressure and $\mathbf{t} \overset{\text{def}}{=} \boldsymbol{\tau} - p\mathbf{1}$ is the deviatoric part of $\boldsymbol{\tau}$, with spectral representation

$$\mathbf{t} = \sum_{A=1}^{3} t_A \, \mathbf{n}_A \otimes \mathbf{n}_A. \tag{10}$$

An isotropic yield function is considered and expressed as

$$F(J_2) = f(J_2) - \sigma_y \tag{11}$$

where J_2 is the second invariant of the deviatoric Kirchhoff stress and σ_y is a material parameter. We also consider the evolutive equation in the form (Simo and Hughes [1], Simo [9])

$$-\frac{1}{2}\mathcal{L}_v \mathbf{b}^e = \dot{\gamma}\mathbf{N}\mathbf{b}^e, \tag{12}$$

where

$$\mathcal{L}_v \mathbf{b}^e = \mathbf{F}\frac{\partial}{\partial t}[(\mathbf{C}^{p-1})]\mathbf{F}^T \tag{13}$$

is the Lie derivative of $\mathbf{b}^e$, $\dot{\gamma}$ is the plastic consistency parameter, and $\mathbf{N} = \partial_{\boldsymbol{\tau}} F$ is the normal to the yield surface with spectral representation

$$\mathbf{N} = \sum_{A=1}^{3} N_A \, \mathbf{n}_A \otimes \mathbf{n}_A. \tag{14}$$

In generalized plasticity at finite strains a limit equation is introduced and expressed as (Auricchio and Taylor [6])

$$h(F)[\mathbf{N} : \dot{\boldsymbol{\tau}}] - \dot{\gamma} = 0, \tag{15}$$

where

$$h(F) = \frac{F}{\delta(\beta - F) + H\beta}, \tag{16}$$

with β and δ being two positive constants with dimensions of stress and $H = H_{iso} + H_{kin}$.

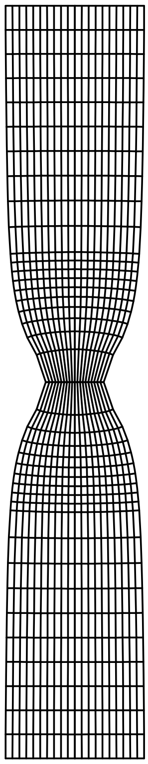

Figure 1: Deformed configuration of the circular bar at an elongation of 26.25 per cent

3 TIME DISCRETE SOLUTION ALGORITHM

A product formula algorithm is considered via an operator split approach for the local problem of evolution. A relative deformation gradient $\mathbf{f}$ is introduced such that

$$\mathbf{F} = \mathbf{f}\,\mathbf{F}_n. \tag{17}$$

Consequently, the operator split approach leads to a trial elastic state in which

$$\mathbf{b}^{e,TR} = \mathbf{f}\,\mathbf{b}^e_n \mathbf{f}^T, \tag{18}$$

and subsequently, via an exponential approximation for the rate equation, a return mapping state in which

$$\mathbf{b}^e = \exp\left[-2\Delta\gamma\mathbf{N}\right]\mathbf{b}^{e,TR}. \tag{19}$$

In the above equation we observe that $\mathbf{b}^e$ and $\mathbf{N}$ have the same spectral decomposition, which implies that also $\mathbf{b}^e$ and $\mathbf{b}^{e,TR}$ have the same spectral decomposition. Consequently $\mathbf{n}_A^{TR} = \mathbf{n}_A$ and equation (19) can be expressed as three scalar equations relative to the space of principal directions

$$\lambda_A^e = \exp\left[-\Delta\gamma\mathbf{N}_A\right]\lambda_A^{e,TR} \tag{20}$$

where $(\lambda_A^{e,TR})^2$ and $\mathbf{n}_A^{TR}$ are the eigenvalues and the eigenvectors of $\mathbf{b}^{e,TR}$. By taking the logarithm of both sides of equation (20) we get

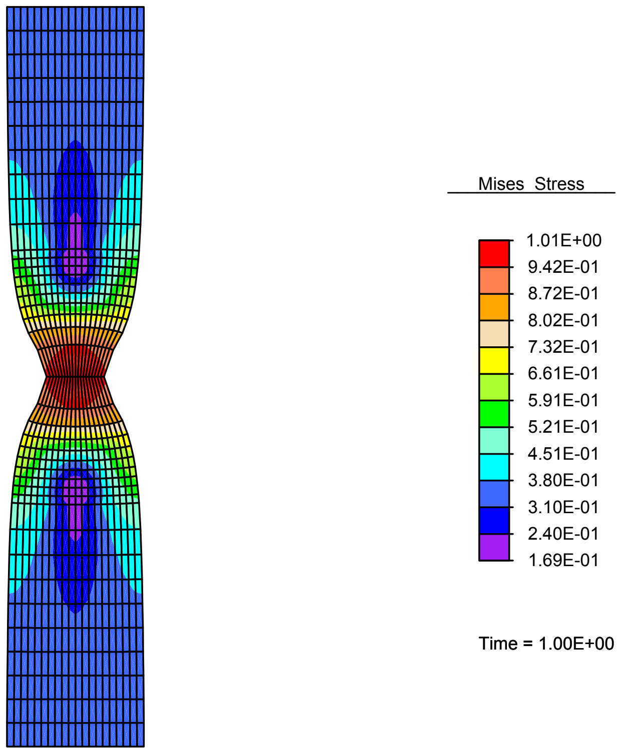

Figure 2: Contour plot of the second invariant of the deviator stress

$$\log[\lambda_A^e] = -\Delta\gamma \mathbf{N}_A + \log[\lambda_A^{e,TR}], \tag{21}$$

and introducing the principal elastic logarithmic strains

$$\varepsilon_A^e = \log[\lambda_A^e], \qquad \varepsilon_A^{e,TR} = \log[\lambda_A^{e,TR}], \tag{22}$$

equation (21) is expressed as

$$\varepsilon_A^e = \varepsilon_A^{e,TR} - \Delta\gamma \mathbf{N}_A, \tag{23}$$

which represents a return mapping algorithm in strain space. For a more detailed description of the algorithmic procedure we refer to De Angelis and Taylor [10].

4 NUMERICAL EXAMPLE

In this example we consider the three-dimensional behaviour of a circular bar subjected to tension. This well-documented problem has been studied by several authors, see e.g. Simo and Hughes [1] and Simo [9]. Due to symmetry only 1/4 of the cylindrical specimen is considered for the discretization with finite elements. Isoparametric 4-node mixed elements are employed in the numerical simulation and implemented in the general purpose finite element program FEAP documented in [11]. An axisymmetric analysis with finite deformations is performed. The mesh consists of 200 elements and 242 nodal points. The

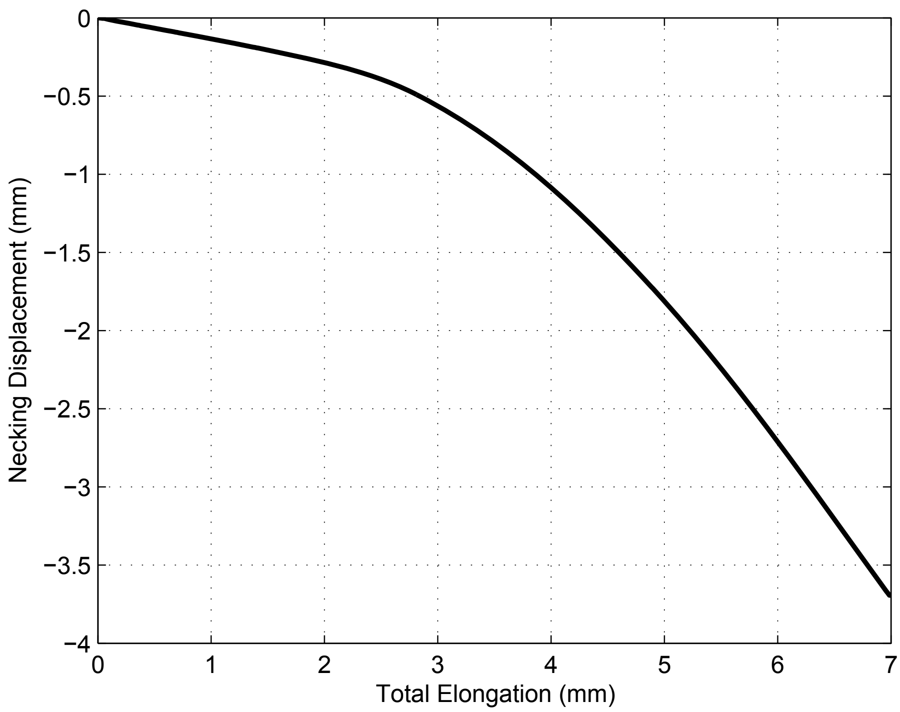

Figure 3: Plot of the necking displacement at the symmetry section versus the elongation of the bar

radius of the cylinder is R = 6.413 mm and the total length of the bar is L = 53.334 mm. The specimen tapers by a small amount to a central location to ensure that the necking will occur in a specified location. In the example a uniform taper to a central radius of R_c = 0.982 R is used. A fit of the hardening data reported in [12] leads to the following material hardening properties for a generalized plasticity model: elastic modulus E = 206.9 GPa, Poisson ratio $\nu = 0.29$, initial flow stress $\sigma_{yo} = 0.45$ GPa, residual flow stress $\sigma_{y\infty} = 0.76$ GPa, $\beta = 0.31$ GPa, $\delta = 0.004$ E, isotropic hardening $H_{iso} = 0.12924$ GPa. A total axial elongation of 14 mm is prescribed, corresponding to an an elongation of 26.25 per cent. This example is quite sensitive to solve as the response involves an unstable behavior of the necking process. In Fig. 1 the deformed configuration of the bar is illustrated at an elongation of 26.25 per cent. The contour plot of the second invariant of the deviator stress is shown in Fig. 2. The necking displacement at the symmetry section versus the elongation of the bar is plotted in Fig. 3.

5 CONCLUSIONS

In the existing literature the model of generalized plasticity has been adopted for the description of material behaviour experiencing inelastic processes in a small strain formulation. In the present paper the model of generalized plasticity has been considered and analyzed with reference to inelastic processes at finite deformations. Accordingly, an effective algorithmic procedure has been proposed for a generalized plasticity model in finite strains elastoplasticity. A product formula algorithm via an operator split approach has been illustrated. A return mapping algorithm has been adopted which has led to a computationally effective solution scheme. The numerical implementation has shown a robust performance in the integration of the model problem. Numerical applications and computational results have been reported with reference to the three-dimensional necking problem of a circular bar subjected to tension.

REFERENCES

[1] Simo, J.C., and Hughes, T.J.R., *Computational Inelasticity.* Springer-Verlag, Berlin, (1998).

[2] Zienkiewicz, O.C., and Taylor, R.L., *The Finite Element Method for Solid and Structural Mechanics.* Elsevier, Oxford, 6th ed., (2005).

[3] Lubliner, J., A simple model of generalized plasticity. *Int. J. Solids Structures* (1991) **28**:769–778.

[4] Lubliner, J., *Plasticity theory.* Macmillan, New York, (1990).

[5] Lubliner, J., Taylor, R.L., and Auricchio, F., A new model of generalized plasticity and its numerical implementation. *Int. J. Solids Structures* (1993) **30**:3171–3184.

[6] Auricchio, F., and Taylor, R.L., Two material models for cyclic plasticity: nonlinear kinematic hardening and generalized plasticity. *Int. J. Plasticity* (1995) **11**:65–98.

[7] Lee, E.H., Elastic-plastic deformation at finite strains. *J. of Applied Mechanics* (1969) **36**:1–6.

[8] Mandel, J., Thermodynamics and plasticity. In: Delgado Dominger, J.J., Nina, M.N.R., Whitelaw, J.H., (Eds.), *Foundations of Continuum Thermodynamics*, pages 283-304. Macmillan, London, (1974).

[9] Simo, J.C., A framework for finite strain elastoplasticity based on maximum plastic dissipation. Part II: Computational aspects. *Comput. Methods Applied Mechanics and Engineerins* (1988) **68**:1–31.

[10] De Angelis, F., and Taylor, R.L., Computational procedures for a generalized plasticity model at finite deformations, *in preparation.*

[11] Taylor, R.L., A finite-element analysis program, *User Manual, Vers: 8.3*, University of California, Berkeley, CA, (2011).

[12] Engelmann, B.E., and Hallquist, J.O., NIKE 2D: A Nonlinear, Implicit, Two-Dimensional Finite Element Code for Solid Mechanics, *Lawrence Livermore National Laboratory*, pages 1-208. University of California, Livermore, CA, (1991).